OPEN ACCESS

Kashf Journal of Multidisciplinary Research
Vol: 02 - Issue 07 (2025)
P-ISSN: 3007-1992 E-ISSN: 3007-200X
https://kjmr.com.pk

NUMERICAL TREATMENT OF TIME-FRACTIONAL ADVECTION DIFFUSION EQUATION VIA B-SPLINE COLLOCATION APPROACH

Ali Usman*
Faculty of Sciences, The Superior University, Lahore, Pakistan

Muhammad Amin
Faculty of Sciences, The Superior University, Lahore, Pakistan

Sagar Hassan
Faculty of Sciences, The Superior University, Lahore, Pakistan

Javeria Kousar
Faculty of Sciences, The Superior University, Lahore, Pakistan

[*]***Corresponding author:*** alirana6415@gmail.com

Article Info

Abstract

In this work, the approximate solution of the time fractional advection-diffusion equation has been explored. A collection of polynomials in pieces that are smooth and governed by a group of control points comprises the B-spline functions. This study develops a numerical method based on Extended Cubic B-spline (ECBS) functions to solve the time fractional advection-diffusion equation (TFADE). The fractional derivative operator has been used in Caputo-Fabrizio sense, which features a non-singular exponential kernel. The finite difference method (FDM) is applied for temporal discretization while ECBS functions are used to approximate spatial derivatives. A thorough analysis of the method's stability and convergence is presented. Numerical results confirm the effectiveness and precision of the proposed scheme, with computed solutions closely aligning with known analytical solutions.

Keywords:

Advection Diffusion Equation, B-Spline Method, Finite Difference Scheme, Caputo-Fabrizio Fractional Derivative, Stability, Convergence.

1. Introduction

Within the fractional calculus (FC) discipline of mathematical analysis, several approaches to determining real or complex number powers are examined. In this extension of classical calculus, the integration and differentiation procedures of fractional order that are not integers are discussed. The development of fractional dynamics, fractional-differential equations (FDE), and other useful domains have depended on the theory of FC since the 19th century. It has recently revealed significant advancements and has grown into an intriguing subject. The FC has several uses in broad and diverse fields of science and engineering, including electrochemistry, fluid dynamics, and electromagnetics. Reports on physical and mechanical processes were made using it.

A number of concepts and their ramifications are being contested by the FC. Chen [1] explored the use of a 2/3-order fractional Laplacian to model turbulent flows, offering a new perspective on turbulence dynamics. The paper presents theoretical insights and conjectures, suggesting that fractional models may better capture the complexity of turbulent systems. Gorenflo and Mainardi [2] provided a foundational treatment of fractional calculus, focusing on integral and differential equations of non-integer order. Their work laid the groundwork for applying fractional models in various scientific fields. Metzler and Klafter [3] presented a comprehensive overview of anomalous diffusion using fractional dynamics, highlighting how random walk models can effectively describe non-standard diffusion processes. Hilfer [4] explored diverse physical applications of fractional calculus, demonstrating its value in modeling complex systems with memory and hereditary properties. Bokhari, Kara, and Zaman [5] analyzed a mathematical model for brain tumor growth, deriving exact solutions and conservation laws to better understand tumor dynamics. Sokolov, Klafter, and Blumen [6] introduced fractional kinetics as a framework for describing anomalous transport phenomena, extending beyond classical kinetic theory. Diethelm & Freed [7] investigate numerical techniques for solving nonlinear fractional differential equations in viscoelasticity, highlighting their effectiveness in modeling complex rheological materials. Li et al. [8] examine a fractional-order delayed model of zooplankton–phytoplankton dynamics, revealing how time delays and memory influence ecological stability. Javaid et al. [9] explore the behavior of fractional Burgers' fluid in a rotating annulus using a power-law kernel, showing how fractional models capture fluid memory effects. Recent studies have utilized fractional calculus to model complex biological systems. Farman et al. applied the Caputo operator to a measles model, Xu et al. developed a fractional HIV-TB coinfection model using real-world data, and Ahmad et al. analyzed tumor-immune interactions through a fractal–fractional framework with dual kernels, highlighting the effectiveness of fractional tools in epidemiological and biomedical modeling [10, 11, 12] are just a few examples of its extensive use. In [13], the proportional Caputo-derivative is examined, along with several useful connections of the beta function and this novel derivative. According to FDEs, fractional models have their positive characteristics and behave effectively, in contrast to typical integer order duplicates. Consequently, it is necessary to examine the solution of these fractional models. Often, there are a lot of FDEs for which there are no analytic solutions. As a result, several recently released papers concentrate on the pursuit of estimated and systematic paths. This study considers the following TFADE for numerical solution.

$$\frac{\partial^{\alpha}}{\partial t^{\alpha}} w(r,t) = P\frac{\partial^{2}}{\partial r^{2}} w(r,t) - Q\frac{\partial w(r,t)}{\partial r} + a(r,t), \qquad p \le r \le q, t_0 \le t \le T, \tag{1}$$

with initial conditions (IC): $w(r,t_0) = w(r)$ (2)

and the Boundary Conditions (BCs): $w(0,t) = \phi_1(t), w(1,t) = \phi_2(t),$ (3)

where $a(r,t)$ is the source term and $0<\alpha<1$. P, $Q>0$ are the diffusion coefficient and average velocity, respectively.

The CFFD with a non-singular and non-local kernel is represented by the $\frac{\partial^{\alpha}}{\partial t^{\alpha}} w(r,t)$ [14]. When applying the Laplace transform to certain bodily problems involving beginning conditions, the CFFD concept offers a notable advantage by providing alternative definitions of derivative operators. When $\alpha=0$, we only recover the original function when the function disappears at the origin. Applications of CFFD have been studied in fields such as the model of heat transfer [14], the physics-entropy [15], transducer's [16], HEV's model [17], cancer medicine [18], smoking model [19], and coronavirus [20].

Numerical and analytical approaches to solving TFADEs have attracted significant research attention. A method for estimating the TFADE based on the moving least-squares (MLS) approach was presented by Mardani et al. [21]. Bu and colleagues [22] proposed a V-cycle cross technique to deal with multi-term TFADEs. Sarboland [23] provided a suitable technique for utilizing the multiquadric quasi-interpolation operator to determine the time fractional PDE. Tian et al. [24] developed the polynomial spectrum-collocation method using Caputo-fractional derivatives (CFDs) to address non-local situations. The SFADE has been developed Zheng et al. [25] using a FEM To solve the space–time Riesz–Caputo FADE. Shen et al. [26] introduced both implicit and explicit difference approaches. Azin et al. provide Chebyshev cardinal functions and modified Legendre to solve the TFADE [27]. An analytic & estimated analysis of two-dimensional TFADE was proposed by Ahmed et al. [28]. The fundamental solutions of T-FADE using the Caputo-Fabrizio operator were obtained by Mirza and Vieru [29]. Baleanu et al.[30] devised the q-homotopic analysis and homotopic perturbation strategies to solve the FADE using CFDs. Rubaab et al.[31] Use integral transform techniques to assess the FADE solution based on time-dependent boundary pulses. The integral transformation approach was established by Rubaab et al. [32] to study the solution of unstable TFADEs. Using the Mittag-Leffler kernel, Attia et al. [33] developed a numerical technique to solve time-fractional advection–diffusion equations based on the Atangana–Baleanu derivative in the Caputo framework.

Many studies have employed splines to solve fractional differential equations because of their ease of use, compact support, good approximation, capacity to obtain estimated solutions to Fractional-Partial-Differential-Equations (FPDEs) of any order, and found piecewise polynomial solutions with degree two continuity. Yaseen et al. [34] offered a capable system for resolving the KG equation with temporal fractions. Using cubic B-spline (CBS) roles, Abbas et al. [35] introduced the unique technique for solving the nonlinear third-order Kortewegde Vries problem. The revised CBS roles-based approach to solving the Allen–Cahn equation was presented by Khalid et al. [36]. Burgers' equations were numerically solved using ABFD by Shafiq et al. [37]. Shafiq et al. have studied the memory impact analysis of the diffusion equation [38]. To solve the Kuramoto–Sivashinsky problem numerically, Iqbal et al. [39] present new quantic B-spline functions. To tackle TFADE, Khalid et al. [40] create a numerical technique based on redefined ECBS functions. Shafiq et al. [41] was presented the CBS functions were presented to solve the TFADE. TFADE numerical solutions using ABFD were provided by Khan et al. [42]. The suggested work is motivated by recent developments in the investigation of TFADE algorithm numerical solutions. A wide range of natural phenomena, such as groundwater contamination, river system thermal pollution, pollutant discharges, and seepage of water, may be described by the ADE. Because of its extensive use, our aim in this work is to solve the TFADE using ECBS. Although a faculty member previously explained TFADE utilizing B. spline approaches, no one has utilized ECBS by a new calculation. The ECBS solves the TFADE using an h-weighted technique. Furthermore, a stability & convergence study of the arrangement is conducted. Providing a solution to certain numerical issues illustrates the usefulness and relevance of the suggested method. We establish that the strategy we have described yields efficient

outcomes by comparison got mathematical outcomes by logical findings. As far as the authors are aware, the proposed algorithm has not yet been explored for solving time-fractional advection–diffusion equations.

That paper has the following shape: Section 3 introduces the current approach, whereas Section 2 provides the preliminary information. Convergence analysis and the stability of the present approach are explained in Sections 4 and 5, respectively. Section 6 looks at the instances' numerical outcomes. In Section 7, the conclusion is then covered.

2. Preliminaries

Definition: Let $v \in H^1(p,q), q > p, 0 < \alpha < 1$, then CFFD with a non-singular Kernel is given as [14]

$$\frac{\partial^\alpha}{\partial u^\alpha} w(r,t) = \frac{M(\alpha)}{2-\alpha} \int_0^1 \frac{\partial^2}{\partial v^2} w(r,u) \exp\left[-\frac{\alpha}{2-\alpha}(t-v) \right] dv, \tag{4}$$

Where Error, editing field codes does not create objects. is the normalizing function that keeps $M(0) = 1$ & $M(1) = 1$, $E_{\varphi,\gamma}(r)$, Mittag-Leffler function holding $E_{\varphi,1}(s) = E_\varphi(s)$, that is provided as:

$$E_{\varphi,\gamma}(s) = \sum_{m=0}^{\infty} \frac{r^m}{\Gamma(\varphi m + \gamma)}.$$

Definition: If $\tilde{g} \in L^2[p,q]$, Parseval's identity is then determined by [43]

$$\begin{aligned} &\sum_{m=0}^{\infty} |\hat{g}(m)|^2 = \int_p^q |\hat{g}(r)|^2 \, dr, \\ &\hat{g}(m) = \int_p^q \tilde{g}(r) e^{2\pi i n s} dr \end{aligned} \tag{5}$$

Each “m” represents its Fourier transformation.

2.1. Basis functions

At the knots, the interval [p, q] is separated into N equivalent sub-intervals.

$r_k = r_0 + kh$, $k = 0:1:N$ and $h = \frac{-(p-q)}{N}$ is the distance b/w knots. The ECBS roles are

$$C_k(r,\eta) = \begin{cases} 4h(1-\eta)(r-r_i)^3 + 3\eta(r-r_i)^4, & r \in [r_i, r_{i+1}), \\ (4-\eta)h^4 + 12h^3(r-r_{i+1}) + 6h^2(2+\eta)(r-r_{i+1})^2 - 12h(r-r_{i+1})^3 - 3\eta(r-r_{i+1})^4, & r \in [r_{i+1}, r_{i+2}), \\ (4-\eta)h^4 + 12h^3(r_{i+3}-r) + 6h^2(2+\eta)(r_{i+3}-r)^2 - 12h(r_{i+3}-r)^3 - 3\eta(r_{i+3}-r)^4, & r \in [r_{i+2}, r_{i+3}), \\ 4h(1-\eta)(r_{i+4}-r)^3 + 3\eta(r_{i+4}-r_i)^4, & r \in [r_{i+3}, r_{i+4}), \\ 0, & otherwise, \end{cases} \tag{6}$$

Where the s variable is denoted by $\eta \in R$. Similar properties to those of the cubic B. spline, such as symmetry, convex hull property, and geometric invariability, are acquired by the ECBS for $-8 \le \eta \le 1$. When $\varsigma = 0$, the ECBS function deteriorates to the CBS role.

Now we take $W(r,t)$ to be the ECBS estimate for $w(r,t)$ in such a way that

$$W(r,t)=\sum_{k=-1}^{N+1}\xi_k^m(t)C_k(r,\eta) \tag{7}$$

Where $\xi_k^m(t)$ stands for the points that need to be calculated at every time-level and $C_k(r,\eta)$ are Extended-CBS functions. As of the ECBS's local provision of property, $C_k(r,\eta)$ is non-zero in $[r_i,r_{i+4})$. Consequently, only three non-zero basis functions are taken into account, $C_{k-1}(r,\eta)$ $C_k(r,\eta)$, and $C_{k+1}(r,\eta)$ for the evaluation at each knot.

Thus, using (6) and (7) we acquire

$$\begin{cases}(w)_k^m=\xi_{k-1}^m\left(\dfrac{4-\eta}{24}\right)+\xi_k^m\left(\dfrac{8+\eta}{12}\right)+\xi_{k+1}^m\left(\dfrac{4-\eta}{24}\right)\\ (w_s)_k^m=\xi_{k-1}^m\left(\dfrac{-1}{2h}\right)+\xi_k^m(0)+\xi_{k+1}^m\left(\dfrac{1}{2h}\right)\\ (w_{ss})_k^m=\xi_{k-1}^m\left(\dfrac{2+\eta}{2h^2}\right)+\xi_k^m\left(-\dfrac{2+\eta}{h^2}\right)+\xi_{k+1}^m\left(\dfrac{2+\eta}{2h^2}\right)\end{cases} \tag{8}$$

3. An explanation of the scheme

This section presents the scheme in both temporal and spatial directions.

3.1. Discretization in time

The discretization of CFFD in (4) is provided by taking an interval [0, T] and splitting it in to grid points $0=t_0<t_1<.....<t_M=T$, where $t_m=M\Delta t$ And m=0, 1,…, M is divided into M equal subintervals with scope of $\Delta t=\dfrac{T}{M}$ at Knot $t=t_{m+1}$ [14, 37, 42].

$$\frac{\partial^\alpha}{\partial t^\alpha}w(r,t_{m+1})=\frac{M(\alpha)}{2-\alpha}\int_0^{t_{m+1}}\frac{\partial^2}{\partial v^2}w(r,v)\exp\left[-\frac{\alpha}{2-\alpha}(t_{m+1}-v)\right]dv,\quad \alpha\in(0,1)$$

$$=\frac{M(\alpha)}{2-\alpha}\sum_{l=0}^{m}\int_{t_l}^{t_{l+1}}\frac{\partial^2}{\partial v^2}w(r,v)\exp\left[-\frac{\alpha}{2-\alpha}(t_{m+1}-v)\right]dv, \tag{9}$$

Eq. (9) is transformed using the forward difference formulation as

$$\frac{\partial^\alpha}{\partial t^\alpha}w(r,t_{m+1})=\frac{M(\alpha)}{2-\alpha}\sum_{l=0}^{m}\frac{w(r,t_{l+1})-2w(r,t_l)+w(r,t_{l-1})}{(\Delta t)^2}\times\int_{t_l}^{t_{l+1}}\exp\left[-\frac{\alpha}{2-\alpha}(t_{m+1}-v)\right]dv+\mu_{\Delta t}^{m+1}$$

$$=\frac{M(\alpha)}{\alpha(\Delta t)^2}\left[1-\exp\left(-\frac{\alpha}{2-\alpha}\Delta t\right)\right]\sum_{l=0}^{m}\left[w(r,t_{m-l+1})-2w(r,t_{m-l})+w(r,t_{m-l-1})\right]\left(\exp\left[-\frac{\alpha}{2-\alpha}(l\Delta t)\right]\right)+\mu_{\Delta t}^{m+1}$$

Hence,

$$\frac{\partial^{\alpha}}{\partial t^{\alpha}} w(r,t_{m+1}) = \frac{\xi M(\alpha)}{\alpha(\Delta t)^2} \sum_{l=0}^{m} j_l \left[w(r,t_{m-l+1}) - w(r,t_{m-l}) \right] + w(r,t_{m-l-1}) + \mu_{\Delta t}^{m+1} \tag{10}$$

Where $\xi = 1 - \exp\left(-\frac{\alpha}{2-\alpha} \Delta t \right)$ *and* $j_l = \exp\left[-\frac{\alpha}{2-\alpha} (l\Delta t) \right]$ and $\mu_{\Delta t}^{m+1}$ was the shortness error, and this is bound, such that.

$$\left| \mu_{\Delta t}^{m+1} \right| \le \sigma (\Delta t)^2 \tag{11}$$

Whereas σ is a constant.

That much is clear.

- $j_l > 0$ and $j_0 = E_1,\ l = 1(1)m,$
- $j_0 > j_l > j_2 > \ldots\ldots > j_l, j_l \to 0$ as $l \to \infty,$
- $\sum_{l=0}^{m} (j_l - j_{l+1}) + j_{m+1} = (E_1 - j_1) + \sum_{l=1}^{m-1} (j_l - j_{l+1}) + j_m = E_1$.

3.2. Discretization of space

The numerical solution to TFADE is now presented. With the help of (10) and scheme, Eq.(1) becomes

$$\begin{aligned} &\frac{\xi M(\alpha)}{\alpha(\Delta t)^2} \sum_{l=0}^{m} j_l \left[w(r,t_{m-l+1}) - 2w(r,t_{m-l}) + w(r,t_{m-l-1}) \right] \\ &= \theta (P w_{rr}(r,t_{m+1}) - Q w_r(r,t_{m+1})) + (1-\theta)(P w_{rr}(r,t_m) - Q w_r(r,t_m)) + a(r,t_{m+1}). \end{aligned} \tag{12}$$

After simplification

$$\sum_{l=0}^{m} j_l \left[w(r,t_{m-l+1}) - 2w(r,t_{m-l}) + w(r,t_{m-l-1}) \right]$$

$$= \frac{\alpha(\Delta t)^2}{\xi M(\alpha)} \theta (P w_{rr}(r,t_{m+1}) - Q w_r(r,t_{m+1})) + (1-\theta)(P w_{rr}(r,t_m) - Q w_r(r,t_m)) + a(r,t_{m+1}).$$

After expanding Σ value

$$j_0 \left[w(r,t_{m+1}) - 2w(r,t_m) + w(r,t_{m-1}) \right] + \sum_{l=1}^{m} j_l \left[w(r,t_{m-l+1}) - 2w(r,t_{m-l}) + w(r,t_{m-l-1}) \right]$$

$$= \frac{\alpha(\Delta t)^2}{\xi M(\alpha)} \theta (P w_{rr}(r,t_{m+1}) - Q w_r(r,t_{m+1})) + (1-\theta)(P w_{rr}(r,t_m) - Q w_r(r,t_m)) + a(r,t_{m+1}).$$

For $\theta = 1$ We discretize (12) along the space discretization as:

$$E_1 w_k^{m+1} - 2E_1 w_k^m + E_1 w_k^{m-1} + \sum_{l=1}^{m} j_l (w_k^{m-l+1} - 2w_k^{m-l} + w_k^{m-l-1}) = \delta P (w_{rr})_k^{m+1} - \delta Q (w_r)_k^{m+1} + \delta a_k^{m+1}$$

$$E_1 w_k^{m+1} - \delta P(w_{rr})_k^{m+1} + \delta Q(w_r)_k^{m+1} = 2E_1 w_k^m - E_1 w_k^{m-1} - \sum_{l=1}^{m} j_l (w_k^{m-l+1} - 2w_k^{m-l} + w_k^{m-l-1}) + \delta a_k^{m+1} \quad (13)$$

where $\delta = \dfrac{\alpha(\Delta t)^2}{\xi M(\alpha)}$, $w_k^m = w(r_k, t_m)$, *and* $a_k^{m+1} = a(r_k, t_{m+1})$.

Using (8) in (13), we get

$$\begin{aligned}
&E_1\left[\xi_{k-1}^{m+1}\left(\frac{4-\eta}{24}\right)+\xi_k^{m+1}\left(\frac{8+\eta}{12}\right)+\xi_{k-1}^{m+1}\left(\frac{4-\eta}{24}\right)\right]-\delta P\left[\xi_{k-1}^{m+1}\left(\frac{2+\eta}{2h^2}\right)+\xi_k^{m+1}\left(-\frac{2+\eta}{h^2}\right)+\xi_{k+1}^{m+1}\left(\frac{2+\eta}{2h^2}\right)\right]\\
&+\delta Q\left[\xi_{k-1}^{m+1}\left(\frac{-1}{2h}\right)+\xi_k^{m+1}(0)+\xi_{k+1}^{m+1}\left(\frac{1}{2h}\right)\right]\\
&=2E_1\left[\xi_{k-1}^{m}\left(\frac{4-\eta}{24}\right)+\xi_k^{m}\left(\frac{8+\eta}{12}\right)+\xi_{k+1}^{m}\left(\frac{4-\eta}{24}\right)\right]-E_1\left[\xi_{k-1}^{m-1}\left(\frac{4-\eta}{24}\right)+\xi_k^{m-1}\left(\frac{8+\eta}{12}\right)+\xi_{k+1}^{m-1}\left(\frac{4-\eta}{24}\right)\right]\\
&-\sum_{l=1}^{m} j_l\left[(\xi_{k-1}^{m-l+1}-2\xi_{k-1}^{m-l}+\xi_{k-1}^{m-l-1})\left(\frac{4-\eta}{24}\right)+(\xi_{k-1}^{m-l+1}-2\xi_{k-1}^{m-l}+\xi_{k-1}^{m-l-1})\left(\frac{8+\eta}{12}\right)\right.\\
&\left.+(\xi_{k-1}^{m-l+1}-2\xi_{k-1}^{m-l}+\xi_{k-1}^{m-l-1})\left(\frac{4-\eta}{24}\right)\right]+\delta a_k^{m+1}.
\end{aligned} \quad (14)$$

After some simplification, we have

$$\begin{aligned}
&\xi_{k-1}^{m+1}\left(E_1 p_1 - \delta P p_4 - \delta Q p_3\right) + \xi_k^{m+1}(E_1 p_2 - \delta P p_5) + \xi_{k+1}^{m+1}\left(E_1 p_1 - \delta P p_4 + \delta Q p_3\right)\\
&= \delta a_k^{m+1} - \sum_{l=1}^{m} j_l[(\xi_{k-1}^{m-l+1} - 2\xi_{k-1}^{m-l} - \xi_{k-1}^{m-l-1})p_1 + (\xi_k^{m-l+1} - 2\xi_k^{m-l} - \xi_k^{m-l-1})p_2 +\\
&(\xi_{k+1}^{m-l+1} - 2\xi_{k+1}^{m-l} - \xi_{k+1}^{m-l-1})p_1] + 2E_1(\xi_{k-1}^{m} p_1 + \xi_k^{m} p_2 + \xi_{k+1}^{m} p_1) - E_1(\xi_{k-1}^{m-1} p_1 + \xi_k^{m-1} p_2 + \xi_{k+1}^{m-1} p_1),
\end{aligned} \quad (15)$$

where $p_1 = \dfrac{4-\eta}{24}$, $p_2 = \dfrac{8+\eta}{12}$, $p_3 = \dfrac{1}{2h}$, $p_4 = \dfrac{2+\eta}{2h^2}$, $p_5 = \dfrac{-(2+\eta)}{h^2}$

There are N+1 linear equations with N+3 nonentities in system (15). For an inimitable solution, two supplementary equations can be derived from BCs (3). Thus, a matrix system of dimensions is obtained as follows:

$$B\xi^{m+1} = R\left(\sum_{l=0}^{m-1}(j_l - j_{l+1})\xi^{m-1} + j_m \xi^0\right) + \delta L^{m+1} \quad (16)$$

where,

$$B = \begin{bmatrix}
p_1 & p_2 & p_1 & & & & & & \\
z_1 & z_2 & z_3 & & & & & & \\
 & z_1 & z_2 & z_3 & & & & & \\
 & & & \ddots & \ddots & \ddots & & & \\
 & & & & & z_1 & z_2 & z_3 & \\
 & & & & & & z_1 & z_2 & z_3 \\
 & & & & & & p_1 & p_2 & p_1
\end{bmatrix},$$

$$C=\begin{bmatrix} 0 & 0 & 0 & & & & & & \\ p_1 & p_2 & p_1 & & & & & & \\ & p_1 & p_2 & p_1 & & & & & \\ & & & \ddots & \ddots & \ddots & & & \\ & & & & & p_1 & p_2 & p_1 & \\ & & & & & & p_1 & p_2 & p_1 \\ & & & & & & 0 & 0 & 0 \end{bmatrix},$$

$$\xi^m=\begin{bmatrix} \xi_{-1}^m & \xi_0^m & \xi_1^m & \cdots & \xi_{N-1}^m & \xi_N^m & \xi_{N+1}^m \end{bmatrix}^T$$

$$L^{m+1}=\begin{bmatrix} \upsilon_1^{m+1} & a_0^{m+1} & a_1^{m+1} & \cdots & a_{N-1}^{m+1} & a_N^{m+1} & \upsilon_2^{m+1} \end{bmatrix}^T$$

where $z_1=E_1p_1-\delta Pp_4-\delta Qp_3, z_2=E_1p_2-\delta Pp_5$ *and* $z_3=E_1p_1-\delta Pp_4+\delta Qp_3$

The initial vector $\xi_0=\begin{bmatrix} \xi_{-1}^m, & \xi_0^m, & \xi_1^m, & \cdots & ,\xi_{N-1}^m, & \xi_{N,}^m & \xi_{N+1}^m \end{bmatrix}^T$ is obtained by using ICs as follows, before using (16):

$$\begin{cases} (W_r)_k^0=w'(r_k), & k=0, \\ (W)_k^0=w(r_k), & k=0:1:N, \\ (W_r)_k^0=w'(r_k), & k=N \end{cases} \tag{17}$$

Eq. (17) is given in matrix form as follows:

$$J\xi_0=U, \tag{18}$$

Where,

$$J=\begin{bmatrix} -p_3 & 0 & p_3 & & & & & & \\ p_1 & p_2 & p_1 & & & & & & \\ & p_1 & p_2 & p_1 & & & & & \\ & & & \ddots & \ddots & \ddots & & & \\ & & & & & p_1 & p_2 & p_1 & \\ & & & & & & p_1 & p_2 & p_1 \\ & & & & & & -p_3 & 0 & p_3 \end{bmatrix}=\begin{bmatrix} w'(r_0) \\ w(r_0) \\ w(r_1) \\ \vdots \\ w(r_{N-1}) \\ w(r_N) \\ w'(r_N) \end{bmatrix}$$

Eq. (18) is easily solved with the aid of an appropriate computing approach. All programming is done using Mathematica 12.

4. Stability

We use the Fourier scheme to examine the stability of the proposed numerical system. Let the numerical growth and analytical factors for the Fourier modes. [37], [40] be denoted by ϑ_k^m *and* $\tilde{\vartheta}_k^m$, respectively. It specifies the mistake $\prod_k^m$ as:

$$\prod_k^m = \vartheta_k^m - \tilde{\vartheta}_k^m, \ k = 1(1) \quad N-1, \quad m = 0,1,\ldots,M. \tag{19}$$

To simplify, we analyze the current method's stability in the absence of a forcing term.

$(a(r,t) = 0)$ [44]. Thus, using Eq.(15), we obtain

$$\begin{aligned}
&\prod_{k-1}^{m+1}[E_1 p_1 - \delta P p_4 - \delta Q p_3] + \prod_k^{m+1}[E_1 p_2 - \delta\xi P p_5] + \prod_{k+1}^{m+1}[E_1 p_1 - \delta P p_4 + \delta Q p_3] \\
&= 2E_1[\prod_{k-1}^m p_1 + \prod_k^m p_2 + \prod_{k+1}^m p_1] - E_1[\prod_{k-1}^{m-1} p_1 + \prod_k^{m-1} p_2 + \prod_{k+1}^{m-1} p_1] \\
&-\sum_{l=1}^{m} j_l[(\prod_{k-1}^{m-l+1} - 2\prod_{k-1}^{m-l} - \prod_{k-1}^{m-l-1})p_1 + (\prod_k^{m-l+1} - 2\prod_{k-1}^{m-l} - \prod_{k-1}^{m-l-1})p_2 + (\prod_{k+1}^{m-l+1} - 2\prod_{k-1}^{m-l} - \prod_{k-1}^{m-l-1})p_1]
\end{aligned} \tag{20}$$

We can inscribe from ICs and BCs

$$\prod_k^0 = w(r_k), \qquad k = 1:1:N, \tag{21}$$

and

$$\prod_0^m = \upsilon_1(t_m), \ \prod_N^m = \upsilon_2(t_m), \qquad m = 0(1)\ M. \tag{22}$$

The grid function is defined as:

$$\prod^m = \begin{cases} \prod_k^m, \ r_k - \dfrac{h}{2} < r \le r_k + \dfrac{h}{2}, \quad k = 1,2,\cdots,N-1 \\ 0, \qquad\qquad p \le r \le \dfrac{2p+h}{2} or \dfrac{2h-h}{2} \le r \le q \end{cases} \tag{23}$$

The Fourier expansion is now expressed as follows:

$$\prod^m(r) = \sum_{n=-\infty}^{\infty} {}^m(n) e^{\frac{2\pi z n x}{q-p}} \tag{24}$$

where,

$$\bar{\upsilon}^m(n) = \frac{1}{q-p}\int_p^q \prod^m(x) e^{\frac{2\pi z n x}{q-p}}\, dx$$

and

$$\prod^m = [\prod_1^m, \prod_2^m, \ldots, \prod_{N-1}^m]^T$$

Using the $\|.\|_2$ norm, we obtain

$$\|\prod^m\|_2 = \left(\sum_{k=1}^{N-1} h\left|\prod_k^m\right|^2\right)^{\frac{1}{2}},$$

$$= \left(\int_p^{p+\frac{h}{2}}\left|\prod^m\right|^2 dr + \sum_{k=1}^{N-1}\int_{r_k-\frac{h}{2}}^{r_k+\frac{h}{2}}\left|\prod^m\right|^2 dr + \int_{q-\frac{h}{2}}^{q}\left|\prod^m\right|^2 dr\right)^{\frac{1}{2}},$$

$$= \left(\int_p^q \left|\prod^m\right|^2 dr\right)$$

Using Parseval's-identity(5), we have [43]

$$\int_p^q \left|\prod^m\right|^2 dr = \sum_{n=-\infty}^{\infty} \left|\bar{\upsilon}^m(n)\right|^2 .$$

Consequently, we obtain

$$\left|\prod^m\right|_2^2 dr = \sum_{n=-\infty}^{\infty} \left|\bar{\upsilon}^m(n)\right|^2 . \tag{25}$$

Next, assume that the Fourier form of the answer is as follows:

$$\prod_k^m = \bar{\upsilon}^m e^{i\beta kh} \tag{26}$$

Where β is any real integer, h is a step size, and $i = \sqrt{-1}$, $\bar{\upsilon}$ is the Fourier coefficient.

Putting (26) into (20), we get

$$\begin{aligned}
&\bar{\upsilon}^{m+1} e^{i\beta(k-1)h}[E_1 p_1 - \delta P p_4 - \delta Q p_3] + \bar{\upsilon}^{m+1} e^{i\beta(k)h}[E_1 p_2 - \delta\xi P p_5] + \bar{\upsilon}^{m+1} e^{i\beta(k+1)h}[E_1 p_1 - \delta P p_4 + \delta Q p_3] \\
&= 2E_1[\bar{\upsilon}^m e^{i\beta(k-1)h} p_1 + \bar{\upsilon}^m e^{i\beta(k)h} p_2 + \bar{\upsilon}^m e^{i\beta(k+1)h} p_1] - E_1[\bar{\upsilon}^{m-1} e^{i\beta(k-1)h} p_1 + \bar{\upsilon}^{m-1} e^{i\beta kh} p_2 + \bar{\upsilon}^{m-1} e^{i\beta(k+1)h} p_1] \\
&- \sum_{l=1}^{m} j_l[(\bar{\upsilon}^{m-l+1} e^{i\beta(k-1)h} - 2\bar{\upsilon}^{m-l} e^{i\beta(k-1)h} - \bar{\upsilon}^{m-l-1} e^{i\beta(k-1)h}) p_1 + (\bar{\upsilon}^{m-l+1} e^{i\beta kh} - 2\bar{\upsilon}^{m-l} e^{i\beta kh} - \bar{\upsilon}^{m-l-1} e^{i\beta kh}) p_2 + \\
&(\bar{\upsilon}^{m-l+1} e^{i\beta(k+1)h} - 2\bar{\upsilon}^{m-l} e^{i\beta(k+1)h} - \bar{\upsilon}^{m-l-1} e^{i\beta(k+1)h}) p_1]
\end{aligned}$$

After compiling the related phrases using the relation $e^{i\beta h} + e^{-i\beta h} = 2\cos(\beta h)$, we obtain:

$$\bar{\upsilon}^{m+1} = \frac{1}{\zeta}\left[\bar{\upsilon}^m - \frac{1}{E_1}\sum_{l=1}^{m} j_l(\bar{\upsilon}^{m-l+1} - \bar{\upsilon}^{m-l}\right] \tag{27}$$

where $\zeta = 1 + \dfrac{12\delta P(2+\eta)\sin^2\left(\dfrac{\beta h}{2}\right) + 6i\delta Q h \sin\beta h}{E_1 h^2 (6 - (4-\eta)\sin^2\left(\dfrac{\beta h}{2}\right)}$. Now it is clear that $\varsigma \geq 1$ *and* $E_1 > 0$.

Lemma 1: If $\bar{\upsilon}^m$ be the answer to Eq. (27). After that $\left|\bar{\upsilon}^m\right| \leq \left|\bar{\upsilon}^0\right|$ *for* $m = 0(1)M$.

Proof

Mathematical induction will be used. In (27), for m=0, we obtain

$$\left|\bar{\upsilon}^1\right| = \frac{1}{\varsigma}\left|\bar{\upsilon}^0\right| \leq \left|\bar{\upsilon}^0\right|, \qquad \varsigma \geq 1.$$

From (27), we obtain

$$\begin{aligned}\left|\bar{\upsilon}^{m+1}\right| &\le \frac{1}{\varsigma}\left|\bar{\upsilon}^{m}\right| - \frac{1}{\varsigma E_1}\sum_{l=1}^{m} j_l\left(\left|\bar{\upsilon}^{m-l+1}\right| - \left|\bar{\upsilon}^{m-l}\right|\right),\\ &\le \frac{1}{\varsigma}\left|\bar{\upsilon}^{0}\right| - \frac{1}{\varsigma E_1}\sum_{l=1}^{m} j_l\left(\left|\bar{\upsilon}^{0}\right| - \left|\bar{\upsilon}^{0}\right|\right),\\ &\le \left|\bar{\upsilon}^{0}\right|.\end{aligned}$$

Theorem 1: The plan that Eq. (15) suggests is constant.

Proof

Applying Lemma I and Eq. (25) to obtain

$$\| \prod^{m} \|_2 \le \| \prod^{0} \|_2, \qquad m = 0,1,\ldots\ldots,M. \tag{28}$$

This technique is therefore unconditionally stable.

5. Convergence

We lead the approach utilized in [45]. to investigate the convergence of the current strategy. Initially, the subsequent theorem is presented as [46], [47].

Theorem 2: Consider $w(r,t) \in C^4[p,q], a \in C^2[p,q]$ and $x = \{p = r_0, r_1, \ldots, r_n = q\}$ be evenly distributed division of $[p,q]$ with $r_i = p + ih, \quad i = 0,1,\ldots,N.$ if $\tilde{w}(r,t)$ be the unique spline for TFADE at the knots $r_i \in x,$ then there is a constant j independent of h s.t. $\forall t \ge 0$ and $i = 0,1,2,$ we obtain

$$\| D^i\left(w(r,t) - \tilde{W}(r,t)\right)\|_\infty \le k_i h^{4-i} \tag{29}$$

Lemma 2: The inequality is held by the ECBS set $\{C_{-1}, C_0, \ldots, C_N, C_{N+1}\}$ shown in Eq.(6)

$$\sum_{i=-1}^{N} |C_i(r,\eta)| \le \frac{7}{4}, \qquad 0 \le r \le 1 \qquad [48] \tag{30}$$

Theorem 3: For TFADE, there is a numerical estimate $W(r,t)$ to analytic solution $w(r,t)$. Besides, if $a \in C^2[0,1]$, then we get

$$\left\|\left(w(r,t) - W(r,t)\right)\right\|_\infty \le \tilde{k}h^2, \qquad \forall t \ge 0, \tag{31}$$

where h is a positive constant that is appropriate for a modest value and independent of h.

Proof

We adopt that the calculated solution to $W(r,t)$ is $\tilde{W}(r,t) = \sum_{i=-1}^{N+1} \vartheta_i^m(t) C_i(r,\eta)$. The triangle inequality is used to obtain

$$\left\|\left(w(r,t) - W(r,t)\right)\right\|_\infty \le \left\|\left(w(r,t) - \tilde{W}(r,t)\right)\right\|_\infty + \left\|\left(\tilde{W}(r,t) - W(r,t)\right)\right\|_\infty.$$

With Theorem II's assistance for $i = 0$, we attain

$$\left\|\left(w(r,t)-W(r,t)\right)\right\|_{\infty} \le k_0 h^4 \left\|\left(\tilde{W}(r,t)-W(r,t)\right)\right\|_{\infty}. \tag{32}$$

The current approach has the following collocation requirements,

$Lw(r_i,t) = LW(r_i,t) = a(r,t), \qquad i = 0(1)N.$

Adopt that $L\tilde{W}(r_i,t) = \tilde{a}(r,t), \qquad i = 0(1)N.$

Consequently, the difference $L(\tilde{W}(r_i,t)-W(r_i,t))$ at any given position m can be expressed as

$$\begin{aligned}
&\mu_{i-1}^{m+1}[E_1 p_1 - \delta P p_4 - \delta Q p_3] + \mu_i^{m+1}[E_1 p_2 - \delta P p_5] + \mu_{i+1}^{m+1}[E_1 p_1 - \delta P p_4 + \delta Q p_3] \\
&= 2E_1[\mu_{i-1}^{m} p_1 + \mu_i^{m} p_2 + \mu_{i+1}^{m} p_1] - E_1[\mu_{i-1}^{m-1} p_1 + \mu_i^{m-1} p_2 + \mu_{i+1}^{m-1} p_1] - \sum_{l=1}^{m} j_l[(\mu_{i-1}^{m-l+1} - 2\mu_{i-1}^{m-l} - \mu_{i-1}^{m-l-1}) p_1 \\
&+ (\mu_i^{m-l+1} - 2\mu_i^{m-l} - \mu_{i-1}^{m-l-1}) p_2 + (\mu_{i+1}^{m-l+1} - 2\mu_{i+1}^{m-l} - \mu_{i-1}^{m-l-1}) p_1] + \frac{\delta a_i^{m+1}}{h^2}.
\end{aligned} \tag{33}$$

Where $\mu_i^m = \xi_i^m - \vartheta_i^m$ for $i = -1, 0, 1, \ldots, N+1$ and

$\Omega_i^m = h^2[a_i^m - \tilde{a}_i^m]$ *for* $i = 0, 1, \ldots, N.$

As stated, the BCs are:

$$\mu_{i-1}^{m+1} p_1 + \mu_i^{m+1} p_2 + \mu_{i+1}^{m+1} p_1 = 0, \ i = 0, N$$

Inequality (29) makes it evident that

$\left|\Omega_i^m\right| = h^2 \left|a_i^m - \tilde{a}_i^m\right| \le kh^4.$

Take $\Omega^m = \max\{\left|\Omega_i^m\right|; 0 \le i \le N\}, \quad e_i^m = \left|\mu_i^m\right|$ and

$e^m = \max\{\left|e_i^m\right|; 0 \le i \le N\}.$

Put $m = 0$ into(33), we get

$$\begin{aligned}
&\mu_{i-1}^{1}[E_1 p_1 - \delta P p_4 - \delta Q p_3] + \mu_i^{1}[E_1 p_2 - \delta P p_5] + \mu_{i+1}^{1}[E_1 p_1 - \delta P p_4 + \delta Q p_3] \\
&= 2E_1[\mu_{i-1}^{0} p_1 + \mu_i^{0} p_2 + \mu_{i+1}^{0} p_1] - E_1[\mu_{i-1}^{0-1} p_1 + \mu_i^{0-1} p_2 + \mu_{i+1}^{0-1} p_1] - \sum_{l=1}^{0} j_l[(\mu_{i-1}^{0-l+1} - 2\mu_{i-1}^{0-l} - \mu_{i-1}^{0-l-1}) p_1 \\
&+ (\mu_i^{0-l+1} - 2\mu_i^{0-l} - \mu_i^{-(l+1)}) p_2 + (\mu_{i+1}^{0-l+1} - 2\mu_{i+1}^{0-l} - \mu_{i+1}^{0-l-1}) p_1] + \frac{\delta a_i^{0+1}}{h^2}, \ i = 0(1)N
\end{aligned}$$

Utilizing IC $e^0 = 0$ the equation above, it becomes

$$\mu_{i-1}^{1}[E_1 p_1 - \delta P p_4 - \delta Q p_3] + \mu_i^{1}[E_1 p_2 - \delta P p_5]$$
$$+\mu_{i+1}^{1}[E_1 p_1 - \delta P p_4 + \delta Q p_3] = \frac{\delta a_i^{1}}{h^2},$$

Now taking absolute value of μ_i^{1} and Ω_i^{1}, we get

$$e_i^{1} \le \frac{6\delta k h^4}{(2+\eta)[E_1 h^2 + 12\delta P] - 6\delta Q h}, \qquad i = 0(1)N.$$

We obtain from BCs the values of e_{-1}^{1} and e_{N+1}^{1}:

$$e_{-1}^{1} \le \frac{20+\eta}{4-\eta}\left[\frac{6\delta k h^4}{(2+\eta)[E_1 h^2 + 12\delta A] - 6\delta B h}\right],$$
$$e_{N+1}^{1} \le \frac{20+\eta}{4-\eta}\left[\frac{6\delta k h^4}{(2+\eta)[E_1 h^2 + 12\delta A] - 6\delta B h}\right],$$

which implies

$$e^{1} \le k_1 h^4.$$

Where k_1 is independent of h.

To illustrate this theorem, we take a mathematical-induction to m. Considering it to be accurate for $j = 1, 2, \ldots, m$ s.t $e_i^{j} \le k_j h^2$ and $k = \max\{k_j; j = 0, 1, 2, \ldots, m\}$. From, (33), we have

$$\mu_{i-1}^{m+1}[E_1 p_1 - \delta P p_4 - \delta P p_3] + \mu_i^{m+1}[E_1 p_2 - \delta P p_5] + \mu_{i+1}^{m+1}[E_1 p_1 - \delta P p_4 + \delta Q p_3]$$
$$= 2E_1[\mu_{i-1}^{m} p_1 + \mu_i^{m} p_2 + \mu_{i+1}^{m} p_1] - E_1[\mu_{i-1}^{m-1} p_1 + \mu_i^{m-1} p_2 + \mu_{i+1}^{m-1} p_1] - j_0 p_1 \mu_{i-1}^{m+1} - 2j_0 p_1 \mu_{i-1}^{m} - j_0 p_1 \mu_{i-1}^{m-1} +$$
$$j_0 p_2 \mu_i^{m+1} - 2j_0 p_2 \mu_i^{m} - j_0 p_2 \mu_{i-1}^{m-1} + j_0 p_1 \mu_{i+1}^{m+1} - 2j_0 p_1 \mu_{i+1}^{m} - j_0 p_1 \mu_{i-1}^{m-1} + (j_1 p_1 \mu_{i-1}^{m} - 2j_1 p_1 \mu_{i-1}^{m-1} - j_1 p_1 \mu_{i-1}^{m-2}$$
$$+ j_1 p_2 \mu_i^{m} - 2j_1 p_2 \mu_i^{m-1} - j_1 p_2 \mu_{i-1}^{m-2} + j_1 p_1 \mu_{i+1}^{m} - 2j_1 p_1 \mu_{i+1}^{m-1} - j_1 p_1 \mu_{i-1}^{m-2}) + (j_2 p_1 \mu_{i-1}^{m-1} - 2j_2 p_1 \mu_{i-1}^{m-2} - j_2 p_1 \mu_{i-1}^{m-3}$$
$$+ j_2 p_2 \mu_i^{m-1} - 2j_2 p_2 \mu_i^{m-2} - j_2 p_2 \mu_{i-1}^{m-3} + j_2 p_1 \mu_{i+1}^{m-1} - 2j_2 p_1 \mu_{i+1}^{m-2} - j_2 p_1 \mu_{i-1}^{m-3}) + \cdots + (j_{m-1} p_1 \mu_{i-1}^{2} - 2j_{m-1} p_1 \mu_{i-1}^{1}$$
$$- j_{m-1} p_1 \mu_{i-1}^{0} + j_{m-1} p_2 \mu_i^{2} - 2j_{m-1} p_2 \mu_i^{1} - j_{m-1} p_2 \mu_{i-1}^{0} + j_{m-1} p_1 \mu_{i+1}^{2} - 2j_{m-1} p_1 \mu_{i+1}^{1} - j_{m-1} p_1 \mu_{i-1}^{0}) +$$
$$(j_m p_1 \mu_{i-1}^{1} - 2j_m p_1 \mu_{i-1}^{0} - j_m p_1 \mu_{i-1}^{-1} + j_m p_2 \mu_i^{1} - 2j_m p_2 \mu_i^{0} - j_m p_2 \mu_{i-1}^{-1} + j_m p_1 \mu_{i+1}^{1} - 2j_m p_1 \mu_{i+1}^{0} - j_m p_1 \mu_{i-1}^{-1}) + \frac{\delta a_i^{m+1}}{h^2}.$$

Then

$$\mu_{i-1}^{m+1}[E_1 p_1 - \delta P p_4 - \delta P p_3] + \mu_i^{m+1}[E_1 p_2 - \delta P p_5] + \mu_{i+1}^{m+1}[E_1 p_1 - \delta P p_4 + \delta Q p_3]$$
$$= -j_0 p_1 \mu_{i-1}^{m+1} - 2j_0 p_1 \mu_{i-1}^{m} - j_0 p_1 \mu_{i-1}^{m-1} +$$
$$j_0 p_2 \mu_i^{m+1} - 2j_0 p_2 \mu_i^{m} - j_0 p_2 \mu_i^{m-1} + j_0 p_1 \mu_{i+1}^{m+1} - 2j_0 p_1 \mu_{i+1}^{m} - j_0 p_1 \mu_{i+1}^{m-1} + (j_1 p_1 \mu_{i-1}^{m} - 2j_1 p_1 \mu_{i-1}^{m-1} - j_1 p_1 \mu_{i-1}^{m-2}$$
$$+ j_1 p_2 \mu_i^{m} - 2j_1 p_2 \mu_i^{m-1} - j_1 p_2 \mu_i^{m-2} + j_1 p_1 \mu_{i+1}^{m} - 2j_1 p_1 \mu_{i+1}^{m-1} - j_1 p_1 \mu_{i+1}^{m-2}) + (j_2 p_1 \mu_{i-1}^{m-1} - 2j_2 p_1 \mu_{i-1}^{m-2} - j_2 p_1 \mu_{i-1}^{m-3}$$
$$+ j_2 p_2 \mu_i^{m-1} - 2j_2 p_2 \mu_i^{m-2} - j_2 p_2 \mu_i^{m-3} + j_2 p_1 \mu_{i+1}^{m-1} - 2j_2 p_1 \mu_{i+1}^{m-2} - j_2 p_1 \mu_{i+1}^{m-3}) + \cdots + (j_{m-1} p_1 \mu_{i-1}^{2} - 2j_{m-1} p_1 \mu_{i-1}^{1}$$
$$- j_{m-1} p_1 \mu_{i-1}^{0} + j_{m-1} p_2 \mu_i^{2} - 2j_{m-1} p_2 \mu_i^{1} - j_{m-1} p_2 \mu_i^{0} + j_{m-1} p_1 \mu_{i+1}^{2} - 2j_{m-1} p_1 \mu_{i+1}^{1} - j_{m-1} p_1 \mu_{i+1}^{0}) +$$
$$(j_m p_1 \mu_{i-1}^{1} - 2j_m p_1 \mu_{i-1}^{0} - j_m p_1 \mu_{i-1}^{-1} + j_m p_2 \mu_i^{1} - 2j_m p_2 \mu_i^{0} - j_m p_2 \mu_i^{-1} + j_m p_1 \mu_{i+1}^{1} - 2j_m p_1 \mu_{i+1}^{0} - j_m p_1 \mu_{i+1}^{-1}) + \frac{\delta a_i^{m+1}}{h^2}.$$

Now applying norms on μ_i^m and a_i^m use the highest possible norm values, μ_{i-1}^m, μ_{i+1}^m and IC $e^0 = 0$ we get

$$e_i^{m+1} \le \frac{6kh^4}{(2+\eta)[E_1h^2+12\delta P]-6\delta Qh}\left[\delta+\sum_{l=0}^{m-1}(j_l-j_{l+1})\right],$$

Likewise, we obtain e_{-1}^{m+1} and e_{N-1}^{m+1} from the BCs as

$$e_{-1}^{m+1} \le \left(\frac{20+\eta}{4-\eta}\right)\frac{6kh^4}{(2+\eta)[E_1h^2+12\delta A]-6\delta Bh}\left[\delta+\sum_{l=0}^{m-1}(j_l-j_{l+1})\right],$$

and

$$e_{N+1}^{m+1} \le \left(\frac{20+\eta}{4-\eta}\right)\frac{6kh^4}{(2+\eta)[E_1h^2+12\delta A]-6\delta Bh}\left[\delta+\sum_{l=0}^{m-1}(j_l-j_{l+1})\right],$$

Thus, for every m, we get

$$e^{m+1} \le kh^2$$

Specifically

$$\tilde{W}(r,t)-W(r,t)=\sum_{i=-1}^{N+1}(\vartheta_i^m-\xi_i^m)C_i(r,\eta).$$

Therefore, applying Lemma II and the aforesaid inequality, we arrive at

$$\|\tilde{W}(r,t)-W(r,t)\|_\infty \le \frac{7}{4}kh^2 \qquad (34)$$

Inequality (32) with(34), provides

$$\|\tilde{W}(r,t)-W(r,t)\|_\infty \le k_0h^4+\frac{7}{4}kh^2=\tilde{k}h^2,$$

$$\tilde{k}=k_0h^2+\frac{7}{4}k.$$

Theorem 4: The TFADE along IC and BCs is convergent

Proof

Consider $w(r,t)$ and $W(r,t)$ are the approximate and analytic solutions of Time Fractional-ADE, respectively. Accordingly, the relation (11) and the above theorem confirms that random constants $\tilde{k}$ and ϱ exist as,

$$\|w(r,t)-W(r,t)\|_\infty \le \tilde{k}h^2+\varrho(\Delta t)^2$$

Thus, the presented method is convergent.

6. Test problems and discussions

This section's implementation of the suggested problem can be used to assess the current scheme's validity using error norms L^2, L^∞ as

$$L^2 = \left\| w(r_k,t) - W(r_k,t) \right\|_2$$
$$= \sqrt{h\sum_{k=0}^{N} \left| w(r_k,t) - W(r_k,t) \right|^2},$$
$$L^\infty = \left\| w(r_k,t) - W(r_k,t) \right\|_\infty$$

Additionally, the convergence order [41] can be computed by

$$\frac{\log\left(\frac{L^\infty(2N)}{L^\infty(N)}\right)}{\log\left(\frac{2N}{N}\right)}.$$

In every problem, the normalizing function $M(\alpha) = 1$ is assumed.

Problem 1: Take a=1 and b=2, solve (1)–(3) using the initial and boundary conditions $w(r) = e^r$, $\phi_1(t) = Et^\alpha$, $\phi_2(t) = eEt^\alpha$, respectively, and take into account the homogeneous source term on [0, 1]. The Mittag-Leffler function is represented by E_φ, while the precise analytical solution [48] is $w(r,t) = e^r E(t^\alpha) \,.\, E_\varphi(s) = \sum_{m=0}^{\infty} \frac{r^m}{\Gamma(\varphi m + 1)}$.

L_∞ and L_2 are compared between MCTB-DQM [48] and the suggested approach based on extended cubic B-spline for various values in Tables 1-3. The accuracy of our method is higher than that of the MCTB-DQM method with $O(\Delta t^3 + h^2)$[48]. By choosing $\alpha = 0.5\ N = 100\ \&\ at\ time\ T = 1$, the comparison at various r values is displayed in Table 4. The comparison of approximated and exact values for a fully implicit scheme is shown in Figure 1.

$$\frac{\partial^\alpha}{\partial t^\alpha} w(r,t) = \frac{\partial^2}{\partial r^2} w(r,t) - \frac{\partial w(r,t)}{\partial r} + a(r,t), \qquad t \in [0,1], r \in [0,1],$$

with initial condition (IC) and the boundary conditions (BCs):

$$w(r,0) = 0 \quad and \quad w(0,t) = w(1,t) = 0$$

Table I: A comparison of the maximum error of problem I at $T = 1, \Delta t = \frac{1}{100}$ & $\alpha = 0.2$

	FDM [48]		Proposed method		
N	L_∞	L_2	L_∞	L_2	**Order**
08	1.4902×10^{-2}	1.0412×10^{-2}	3.1949×10^{-6}	2.9348×10^{-6}	……

16	3.8827×10^{-3}	2.6898×10^{-3}	9.0501×10^{-7}	8.7103×10^{-7}	1.8260
32	1.0156×10^{-3}	6.6522×10^{-4}	2.4780×10^{-8}	2.2130×10^{-8}	5.1912
64	2.5720×10^{-4}	1.4842×10^{-4}	6.3839×10^{-8}	5.9031×10^{-8}	1.9635
128	6.3504×10^{-5}	2.2129×10^{-5}	9.4751×10^{-9}	9.9734×10^{-9}	2.6877

Table II: A comparison of the maximum error of problem I at $T = 1$, $\Delta t = \frac{1}{100}$ & $\alpha = 0.5$

	FDM [48]		**Proposed method**		
N	L_∞	L_2	L_∞	L_2	**Order**
08	6.3092×10^{-3}	4.4047×10^{-3}	6.3401×10^{-6}	4.3211×10^{-6}	……
16	1.6452×10^{-3}	1.1394×10^{-3}	7.9944×10^{-7}	5.2209×10^{-7}	1.9081
32	4.3121×10^{-4}	$2.8317e \times 10^{-4}$	5.0679×10^{-7}	3.2439×10^{-7}	1.8542
64	1.0956×10^{-4}	6.4521×10^{-4}	8.3292×10^{-8}	7.5078×10^{-8}	2.0593
128	2.7227×10^{-5}	1.0443×10^{-5}	7.1426×10^{-8}	2.3544×10^{-8}	2.1304

Table III: A comparison of the maximum error of problem I at $T = 1$, $\Delta t = \frac{1}{100}$ & $\alpha = 0.8$

	FDM [48]		**Proposed method**		
N	L_∞	L_2	L_∞	L_2	**Order**
08	4.1559×10^{-3}	2.9052×10^{-3}	2.7015×10^{-6}	1.4218×10^{-6}	……
16	1.0852×10^{-3}	7.5335×10^{-4}	7.0223×10^{-7}	5.2491×10^{-7}	1.8173
32	2.8491×10^{-4}	1.8911×10^{-4}	6.8039×10^{-7}	4.3076×10^{-7}	2.1081
64	7.2683×10^{-5}	4.4967×10^{-5}	5.2991×10^{-8}	3.4729×10^{-8}	1.9916
128	1.8220×10^{-5}	8.7572×10^{-6}	8.6339×10^{-8}	5.7703×10^{-8}	1.9979

Table IV: A comparison of the exact solution & approximated solution at T = 1, h = $\frac{1}{1000}$, N=100, $\alpha = 0.5$ and $\eta = 0.00001$ for problem I

r	**Exact Solutions**	**Approximate solutions**	**Errors**
0.1	5.535779114478685	5.535779116592377	$2.1136923322728762 \times 10^{-9}$

0.2	6.117982086212403	6.117982072209552	1.4002851322914012 x10^{-8}
0.3	6.761415878989728	6.761415845475604	3.351412392049724x10^{-8}
0.4	7.472520194474339	7.472520149457045	4.5017293892613 x10^{-8}
0.5	8.258412003666022	8.258411962222271	4.144331278155278 x10^{-8}
0.6	9.126956775938526	9.126956754832165	2.110636110330688 x10^{-8}
0.7	10.086847199300735	10.086847210385214	1.1084479112355439 x10^{-8}
0.8	11.14769017973997	11.147690221970283	4.223031346839434 x10^{-8}
0.9	12.320102990366102	12.320103040206876	4.984077328629155 x10^{-8}

Piecewise solution of Problem 1

$$w(r,t)=\begin{cases}
2.729277964441845\times10^{(-21)}+r(2.0123439294442163+r(-0.06575695898575865 \\
+(1.238435969207705-6.4128142436886675r)r)), & if\ r\in[0.00,0.01) \\
-0.03373551437930211+r(2.696106266647739+r(-4.921162268441179 \\
+(14.740552539774342-16.594358597374196r)r)), & if\ r\in[0.01,0.02) \\
-0.565764802877835+r(8.106471656532946+r(-24.24284366661641 \\
+(41.925852772138455-27.23284722449995r)r)), & if\ r\in[0.02,0.03) \\
-3.18092471146921+r(25.79623209113032+r(-66.20039698373068 \\
+(80.98155670997653-37.18194751375938r)r)), & if\ r\in[0.03,0.04) \\
-11.10896340955324+r(65.89070591385746+r(-137.14566824258077 \\
+(129.97160954364062-46.21591429375769r)r)), & if\ r\in[0.04,0.05) \\
-29.433017927735364+r(139.70882262444684+r(-240.87507446471272 \\
+(186.3986954656898-54.11188297696924r)r)), & if\ r\in[0.05,0.06) \\
-64.89928800300447+r(258.0962741725207+r(-378.1484058496071 \\
+(247.32121409266165-60.67543770792986r)r)), & if\ r\in[0.06,0.07) \\
-125.27934484008802+r(429.57483266368854+r(-546.3591282606212 \\
+(309.46314258501206-65.74496178807499r)r)), & if\ r\in[0.07,0.08) \\
-218.28152815780413+r(658.448695935278+r(-739.3893049585749 \\
+(369.3384540958532-69.19562671407039r)r, & if\ r\in[0.08,0.09) \\
-350.0548785760893+r(943.016031229532+r(-947.6619653336547 \\
+(423.38511510104854-70.9424656632466r)r, & if\ r\in[0.09,0.10)
\end{cases}$$

$$w(r,t)=\begin{cases}
-523.3764212740198+r(1274.0357944057796+r(-1158.3956916160714 \\
+\left(468.1042007197375-70.94246566324341r\right)r, & if\ r\in[0.10,0.11) \\
-735.6566859547802+r(1633.5930130110391+r(-1356.0571544512532 \\
+\left(500.19943608598805-69.19562671406788r\right)r, & if\ r\in[0.11,0.12) \\
-976.9358097288441+r(1994.490334518192+r(-1522.9983076332428 \\
+\left(516.7124132708377-65.74496178807703r\right)r)), & if\ r\in[0.12,0.13) \\
-1228.0703419369383+r(2320.270241201615+r(-1640.256280279682 \\
+\left(515.1488233336713-60.67543770793236r\right)r)), & if\ r\in[0.13,0.14) \\
-1459.3263126475176+r(2565.941811845245+r(-1688.4860278078995 \\
+\left(493.59128066373887-54.11188297696958r\right)r, & if\ r\in[0.14,0.15) \\
-1629.5952132142775+r(2679.449535526539+r(-1648.9888537741645 \\
+\left(450.79469775317193-46.21591429375735r\right)r)), & if\ r\in[0.15,0.16) \\
-1686.4345577465792+r(2603.880352527078+r(-1504.793883012033 \\
+\left(386.2605759115868-37.18194751376035r\right)r)), & if\ r\in[0.16,0.17) \\
-1567.128112843262+r(2280.3978476968005+r(-1241.7655634001494 \\
+\left(300.2921983351812-27.23284722450279r\right)r)), & if\ r\in[0.17,0.18) \\
-1199.5253294508366+r(1649.8912975390049+r(-848.6732554375558 \\
+\left(193.79030770244026-16.594358597377038r\right)r)), & if\ r\in[0.18,0.19) \\
-580.5941484021532+r(757.0821709094016+r(-368.14541102786825 \\
+\left(79.34736449803222-6.412814243689297r\right)r)), & if\ r\in[0.19,0.20).
\end{cases}$$

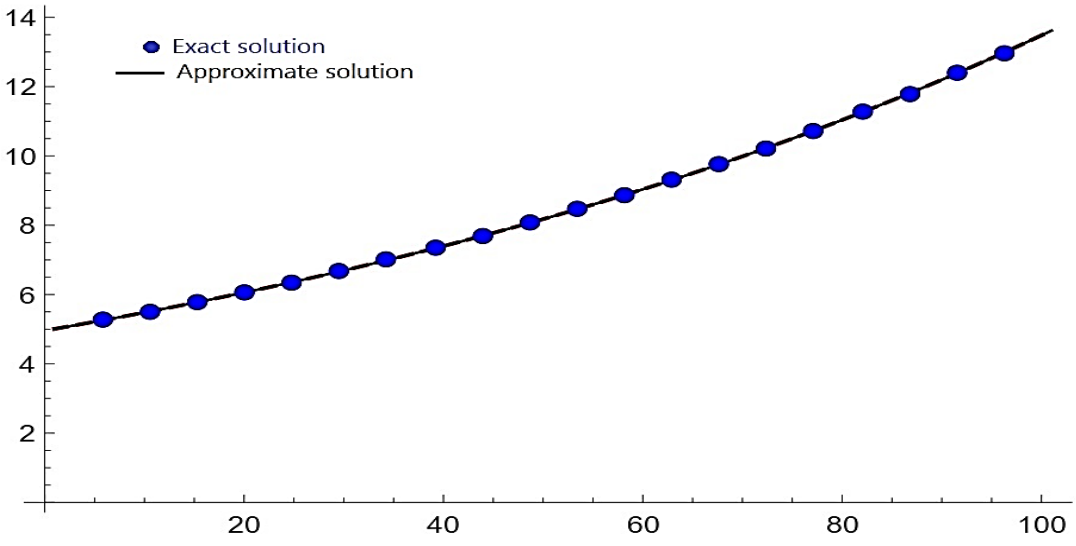

Fig. 1. Comparison graph for exact and approximated values

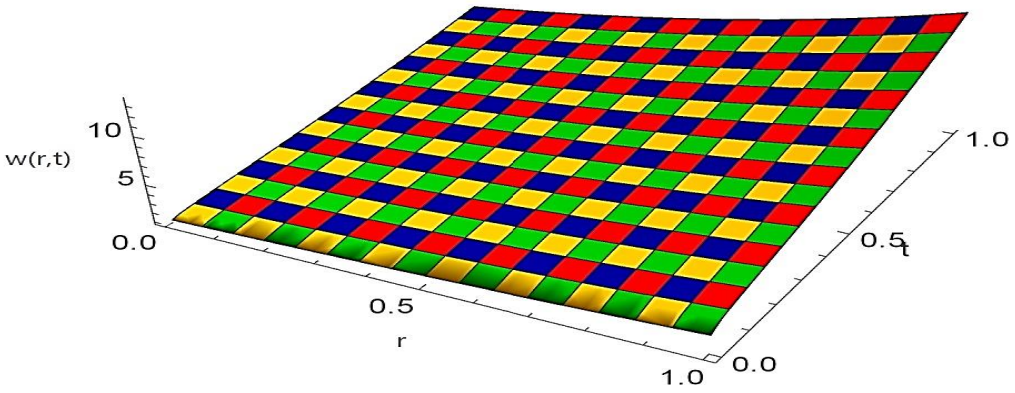

Fig. 2. Plot for the exact solution

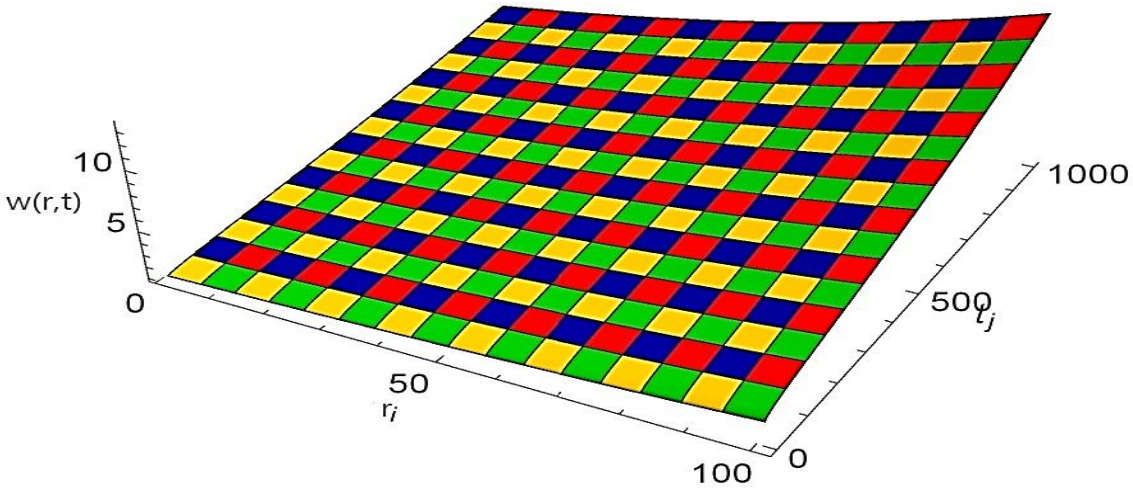

Fig. 3. Plot for the approximated solution

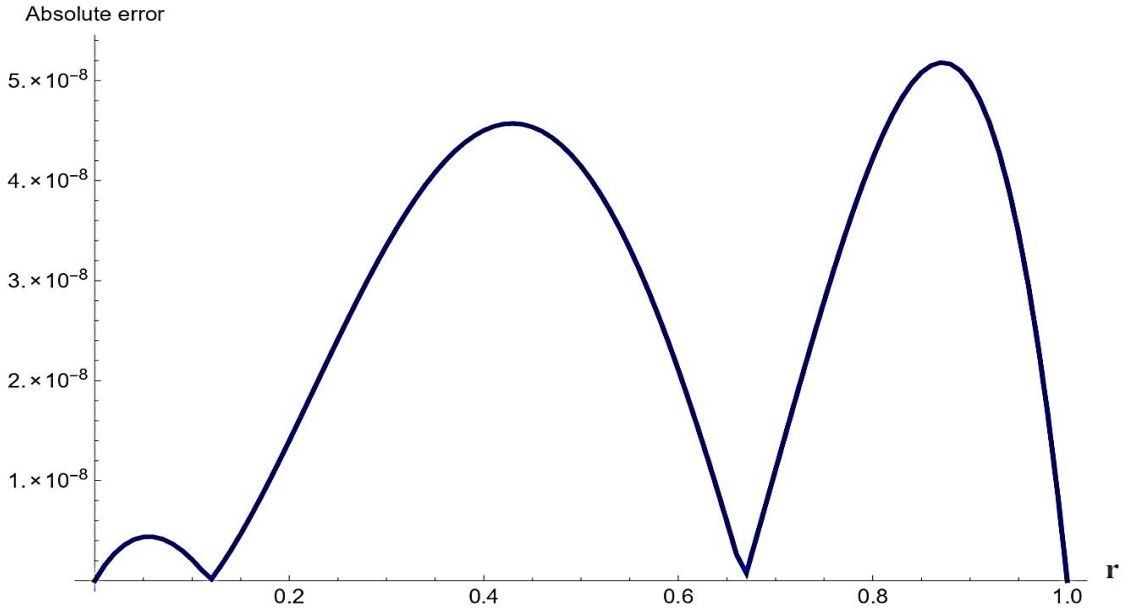

Fig. 4. Graph for absolute error

Problem 2: The homogeneous source term is $a(r,t)=\frac{2t^{2-\alpha}\sin 2\pi r}{\Gamma(3-\alpha)}+4\pi^2t^2\sin(2\pi x)$ on [0, 1] when we solve (1)-(3) with initial and boundary conditions $w(r)=0$, $\phi_1(t)=0$, $\phi_2(t)=0$ respectively, for a=1,b=2. The precise analytical solution [48] is $w(r,t)=t^2\sin(2\pi r)$

The errors between the estimated and exact analytical solutions at various knots corresponding to $N = 100, \alpha = 0.5, \lambda = -0.00065, \Delta t = \frac{1}{100}$, and $T = 1$. are shown in Table 5. The absolute error for Problem 2 for $N = 50, \alpha = 0.3, \Delta t = 0.1$, and $T = 10$ is displayed in Table 6. all the graphical results can also be seen in Figs. 5, 6, 7, and 8.

Table V: A comparison between the approximated and exact solutions at various knots

s	Exact Solutions	Approximate solutions	Absolute Errors
0.1	0.5877852522924731	0.5877852522911452	$1.3279377597541497\text{x}10^{-12}$
0.2	0.9510565162951535	0.9510565162910587	$4.094835581724965\text{x}10^{-12}$
0.3	0.9510565162951535	0.9510565162879967	$7.156830683641147\ \text{x}10^{-12}$
0.4	0.5877852522924731	0.5877852522831861	$9.287015600989434\text{x}10^{-12}$
0.5	0.0	$9.637346476409903\text{x}10^{-12}$	$9.637346476409903\text{x}10^{-12}$
0.6	0.5877852522924731	0.5877852523005364	$8.063216760945124\text{x}10^{-12}$
0.7	0.9510565162951535	0.951056516300331	$5.177414053036955\ \text{x}10^{-12}$
0.8	0.9510565162951535	0.9510565162972706	$2.117084285657711\ \text{x}10^{-12}$
0.9	0.5877852522924731	0.5877852522925808	$1.0769163338864018\text{x}10^{-13}$

Table VI: A comparison between the approximated and exact solutions at various knots

s	Exact Solutions	Approximate solutions	Absolute Errors
0.1	0.5877852522924731	0.5877852522923219	$1.5121237595394632\text{x}10^{-13}$
0.2	0.9510565162951535	0.951056516293149	$2.00450767096072\text{x}10^{-12}$
0.3	0.9510565162951535	0.9510565162904001	$4.753419879932608\ \text{x}10^{-12}$
0.4	0.5877852522924731	0.5877852522851764	$7.296718784743916\text{x}10^{-12}$
0.5	0.0	$-8.633243425704151\ \text{x}10^{-12}$	$8.633243425704151\ \text{x}10^{-12}$
0.6	-0.5877852522924731	-0.5877852523007171	$8.2439610693541\text{x}10^{-12}$
0.7	-0.9510565162951535	-0.9510565163014426	$6.289080367594124\ \text{x}10^{-12}$
0.8	-0.9510565162951535	-0.9510565162986995	$3.5459413183502875\ \text{x}10^{-12}$
0.9	-0.5877852522924731	-0.5877852522935882	$1.1151080059335072\ \text{x}10^{-13}$

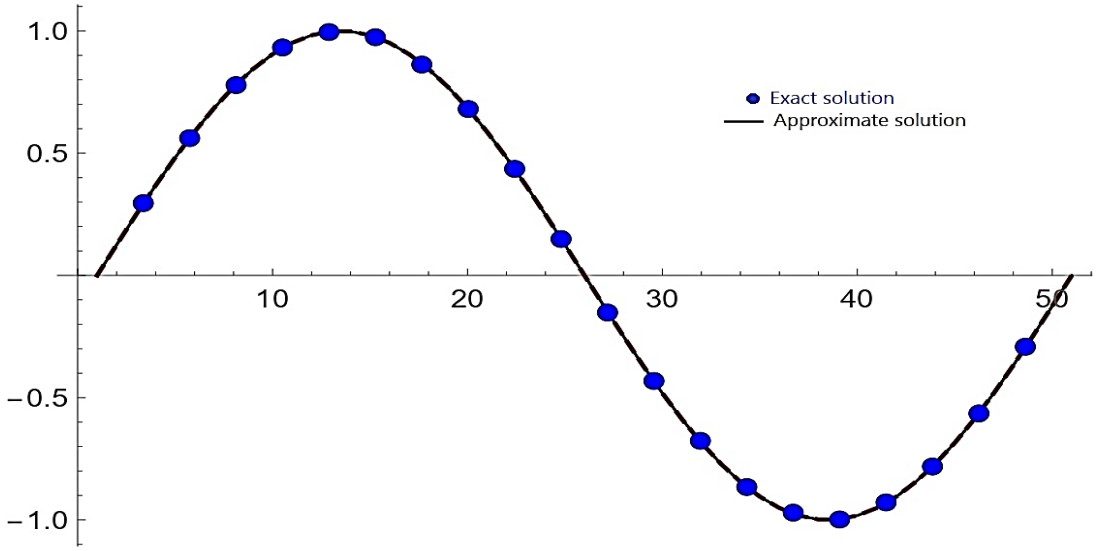

Fig. 5. Comparison graph for exact and approximated values

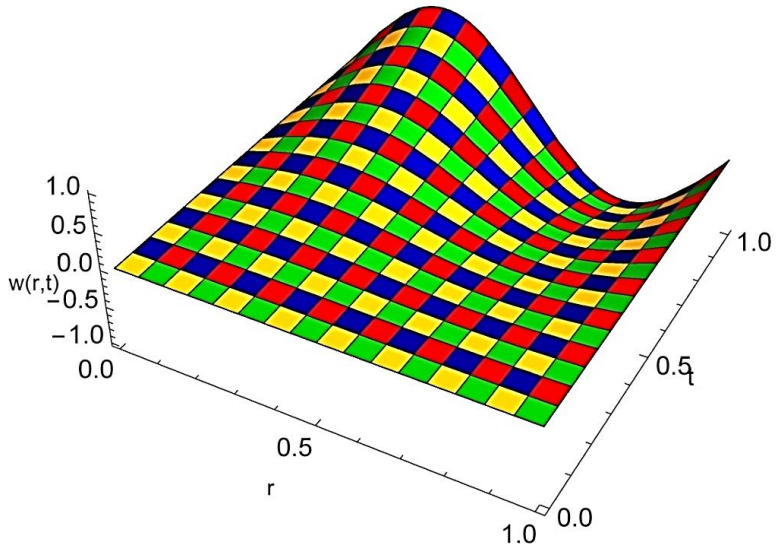

Fig. 6. Plot for the exact solutions

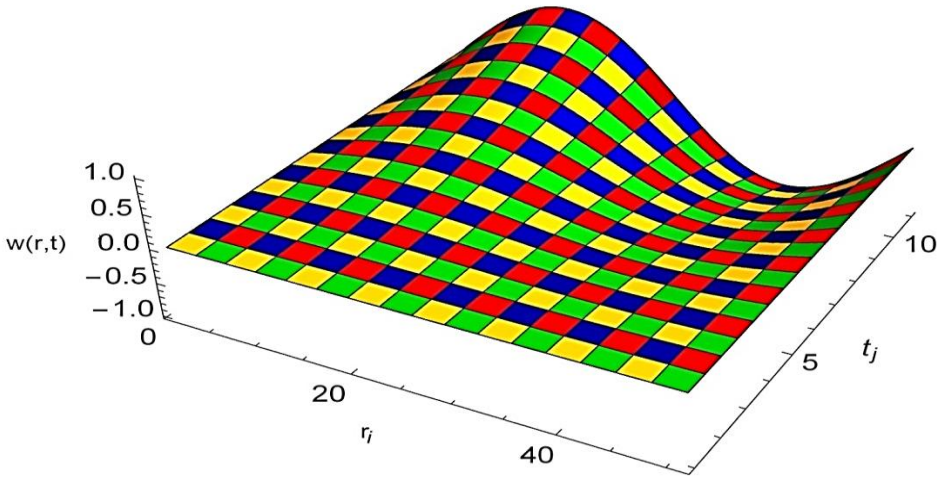

Fig. 7. Plot for the approximated solutions

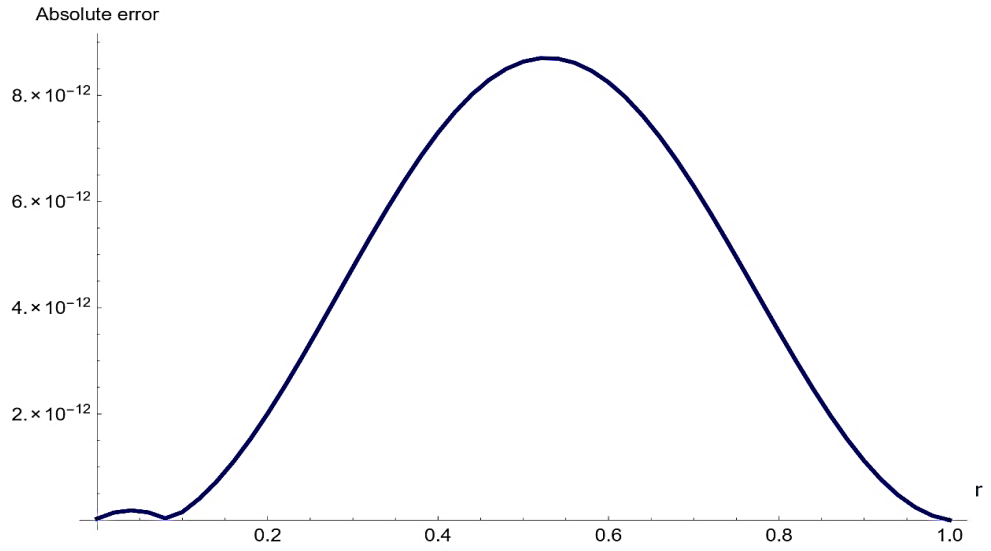

Fig. 8. Graph for absolute error

Conclusion

In this research, a computational technique has been developed using the ECBS method alongside the CFFD scheme to address time-fractional advection–diffusion equations (TFADE). The spatial derivatives are approximated through ECBS basis functions, while the time domain is discretized using a finite difference approach. The method is shown to be stable, achieving second-order accuracy in both space and time, with convergence rates of $O(h)^2$ and $O(\Delta t)^2$, respectively. Several numerical examples have been tested to demonstrate the method's reliability and precision, outperforming previously published techniques. Some extensions of this work remain for future investigation. The ECBS method holds potential for tackling more complex problems, such as space-fractional equations, variable-order systems, and higher-dimensional fractional PDEs. It may also prove effective for equations involving alternative fractional operators.

Authors contributions

Each author made an equal contribution to this piece. The final manuscript was reviewed and approved by all writers.

Declaration of Competing Interest

The authors declare that there are no financial or personal interests that could have impacted the integrity of the research presented in this work.

Reference

[1] W. Chen, "A speculative study of 2⁄3-order fractional Laplacian modeling of turbulence: Some thoughts and conjectures," Chaos: An Interdisciplinary Journal of Nonlinear Science, vol. 16, no. 2, 2006.

[2] R. Gorenflo and F. Mainardi, Fractional calculus: integral and differential equations of fractional order. Springer, 1997.

[3] R. Metzler and J. Klafter, "The random walk's guide to anomalous diffusion: a fractional dynamics approach," Phys Rep, vol. 339, no. 1, pp. 1–77, 2000.

[4] R. Hilfer, Applications of fractional calculus in physics. World scientific, 2000.

[5] A. H. Bokhari, A. H. Kara, and F. D. Zaman, "On the solutions and conservation laws of the model for tumor growth in the brain," J Math Anal Appl, vol. 350, no. 1, pp. 256–261, 2009.

[6] I. M. Sokolov, J. Klafter, and A. Blumen, "Fractional kinetics," Phys Today, vol. 55, no. 11, pp. 48–54, 2002.

[7] K. Diethelm and A. D. Freed, "On the solution of nonlinear fractional-order differential equations used in the modeling of viscoplasticity," in Scientific computing in chemical engineering II: computational fluid dynamics, reaction engineering, and molecular properties, Springer, 1999, pp. 217–224.

[8] P. Li, R. Gao, C. Xu, Y. Li, A. Akgül, and D. Baleanu, "Dynamics exploration for a fractional-order delayed zooplankton–phytoplankton system," Chaos Solitons Fractals, vol. 166, p. 112975, 2023.

[9] M. Javaid, M. Tahir, M. Imran, D. Baleanu, A. Akgül, and M. A. Imran, "Unsteady flow of fractional Burgers' fluid in a rotating annulus region with power law kernel," Alexandria Engineering Journal, vol. 61, no. 1, pp. 17–27, 2022.

[10] M. Farman, A. Shehzad, A. Akgül, D. Baleanu, and M. D. la Sen, "Modelling and analysis of a measles epidemic model with the constant proportional Caputo operator," Symmetry (Basel), vol. 15, no. 2, p. 468, 2023.

[11] C. Xu, Z. Liu, Y. Pang, A. Akgül, and D. Baleanu, "Dynamics of HIV-TB coinfection model using classical and Caputo piecewise operator: A dynamic approach with real data from South-East Asia, European and American regions," Chaos Solitons Fractals, vol. 165, p. 112879, 2022.

[12] S. Ahmad, A. Ullah, A. Akgül, and D. Baleanu, "Theoretical and numerical analysis of fractal fractional model of tumor-immune interaction with two different kernels," Alexandria Engineering Journal, vol. 61, no. 7, pp. 5735–5752, 2022.

[13] A. Akgül and D. Baleanu, "Analysis and applications of the proportional Caputo derivative," Adv Differ Equ, vol. 2021, pp. 1–12, 2021.

[14] M. Shafiq, M. Abbas, H. Emadifar, A. S. M. Alzaidi, T. Nazir, and F. Aini Abdullah, "Numerical investigation of the fractional diffusion wave equation with exponential kernel via cubic B-Spline approach," PLoS One, vol. 18, no. 12, p. e0295525, 2023.

[15] B. S. T. Alkahtani, "Chua's circuit model with Atangana–Baleanu derivative with fractional order," Chaos Solitons Fractals, vol. 89, pp. 547–551, 2016.

[16] J. F. Gómez-Aguilar, "Irving–Mullineux oscillator via fractional derivatives with Mittag-Leffler kernel," Chaos Solitons Fractals, vol. 95, pp. 179–186, 2017.

[17] D. G. Prakasha, P. Veeresha, and H. M. Baskonus, "Analysis of the dynamics of hepatitis E virus using the Atangana-Baleanu fractional derivative," The European Physical Journal Plus, vol. 134, no. 5, p. 241, 2019.

[18] V. F. Morales-Delgado, J. F. Gómez-Aguilar, K. Saad, and R. F. Escobar Jiménez, "Application of the Caputo-Fabrizio and Atangana-Baleanu fractional derivatives to mathematical model of cancer chemotherapy effect," Math Methods Appl Sci, vol. 42, no. 4, pp. 1167–1193, 2019.

[19] S. Uçar, E. Uçar, N. Özdemir, and Z. Hammouch, "Mathematical analysis and numerical simulation for a smoking model with Atangana–Baleanu derivative," Chaos Solitons Fractals, vol. 118, pp. 300–306, 2019.

[20] S. Kumar, J. Cao, and M. Abdel-Aty, "A novel mathematical approach of COVID-19 with non-singular fractional derivative," Chaos Solitons Fractals, vol. 139, p. 110048, 2020.

[21] A. Mardani, M. R. Hooshmandasl, M. H. Heydari, and C. Cattani, "A meshless method for solving the time fractional advection–diffusion equation with variable coefficients," Computers & mathematics with applications, vol. 75, no. 1, pp. 122–133, 2018.

[22] W. Bu, X. Liu, Y. Tang, and J. Yang, "Finite element multigrid method for multi-term time fractional advection diffusion equations," International Journal of Modeling, Simulation, and Scientific Computing, vol. 6, no. 01, p. 1540001, 2015.

[23] M. Sarboland, "Numerical solution of time fractional partial differential equations using multiquadric quasi-interpolation scheme," European Journal of Computational Mechanics, vol. 27, no. 2, pp. 89–108, 2018.

[24] W. Tian, W. Deng, and Y. Wu, "Polynomial spectral collocation method for space fractional advection–diffusion equation," Numer Methods Partial Differ Equ, vol. 30, no. 2, pp. 514–535, 2014.

[25] Y. Zheng, C. Li, and Z. Zhao, "A note on the finite element method for the space-fractional advection diffusion equation," Computers & Mathematics with Applications, vol. 59, no. 5, pp. 1718–1726, 2010.

[26] S. Shen, F. Liu, and V. Anh, "Numerical approximations and solution techniques for the space-time Riesz–Caputo fractional advection-diffusion equation," Numer Algorithms, vol. 56, pp. 383–403, 2011.

[27] H. Azin, F. Mohammadi, and M. H. Heydari, "A hybrid method for solving time fractional advection–diffusion equation on unbounded space domain," Adv Differ Equ, vol. 2020, pp. 1–10, 2020.

[28] N. Ahmed, N. A. Shah, and D. Vieru, "Two-dimensional advection–diffusion process with memory and concentrated source," Symmetry (Basel), vol. 11, no. 7, p. 879, 2019.

[29] I. A. Mirza and D. Vieru, "Fundamental solutions to advection–diffusion equation with time-fractional Caputo–Fabrizio derivative," Computers & Mathematics with Applications, vol. 73, no. 1, pp. 1–10, 2017.

[30] D. Baleanu, B. Agheli, and M. M. Al Qurashi, "Fractional advection differential equation within Caputo and Caputo–Fabrizio derivatives," Advances in Mechanical Engineering, vol. 8, no. 12, p. 1687814016683305, 2016.

[31] Q. Rubbab, I. A. Mirza, and M. Qureshi, "Analytical solutions to the fractional advection-diffusion equation with time-dependent pulses on the boundary," AIP Adv, vol. 6, no. 7, 2016.

[32] Q. Rubbab, M. Nazeer, F. Ahmad, Y.-M. Chu, M. I. Khan, and S. Kadry, "Numerical simulation of advection–diffusion equation with caputo-fabrizio time fractional derivative in cylindrical domains: Applications of pseudo-spectral collocation method," Alexandria Engineering Journal, vol. 60, no. 1, pp. 1731–1738, 2021.

[33] N. Attia, A. Akgül, D. Seba, and A. Nour, "On solutions of time-fractional advection–diffusion equation," Numer Methods Partial Differ Equ, vol. 39, no. 6, pp. 4489–4516, 2023.

[34] M. Yaseen, M. Abbas, and B. Ahmad, "Numerical simulation of the nonlinear generalized time-fractional Klein–Gordon equation using cubic trigonometric B-spline functions," Math Methods Appl Sci, vol. 44, no. 1, pp. 901–916, 2021.

[35] M. Abbas, M. K. Iqbal, B. Zafar, and S. B. M. Zin, "New cubic b-spline approximations for solving non-linear third-order korteweg-de vries equation," Indian J. Sci. Technol, vol. 12, no. 15, pp. 1–9, 2019.

[36] N. Khalid, M. Abbas, M. K. Iqbal, and D. Baleanu, "A numerical investigation of Caputo time fractional Allen–Cahn equation using redefined cubic B-spline functions," Adv Differ Equ, vol. 2020, no. 1, p. 158, 2020.

[37] M. Shafiq, M. Abbas, F. A. Abdullah, A. Majeed, T. Abdeljawad, and M. A. Alqudah, "Numerical solutions of time fractional Burgers' equation involving Atangana–Baleanu derivative via cubic B-spline functions," Results Phys, vol. 34, p. 105244, 2022.

[38] M. Shafiq, F. A. Abdullah, M. Abbas, A. Sm Alzaidi, and M. B. Riaz, "Memory effect analysis using piecewise cubic B-spline of time fractional diffusion equation," Fractals, vol. 30, no. 08, p. 2240270, 2022.

[**39**] M. K. Iqbal, M. Abbas, T. Nazir, and N. Ali, "Application of new quintic polynomial B-spline approximation for numerical investigation of Kuramoto–Sivashinsky equation," Adv Differ Equ, vol. 2020, pp. 1–21, 2020.

[40] N. Khalid, M. Abbas, M. K. Iqbal, J. Singh, and A. I. M. Ismail, "A computational approach for solving time fractional differential equation via spline functions," Alexandria Engineering Journal, vol. 59, no. 5, pp. 3061–3078, 2020.

[41] M. Shafiq, M. Abbas, K. M. Abualnaja, M. J. Huntul, A. Majeed, and T. Nazir, "An efficient technique based on cubic B-spline functions for solving time-fractional advection diffusion equation involving Atangana–Baleanu derivative," Eng Comput, vol. 38, no. 1, pp. 901–917, 2022.

[42] B. Khan, M. Abbas, A. S. M. Alzaidi, F. A. Abdullah, and M. B. Riaz, "Numerical solutions of advection diffusion equations involving Atangana–Baleanu time fractional derivative via cubic B-spline approximations," Results Phys, vol. 42, p. 105941, 2022.

[43] J. R. Poulin, Calculating Infinite Series Using Parseval's Identity. The University of Maine, 2020.

[44] A. R. Mitchell and D. F. Griffiths, "The finite difference method in partial differential equations," A Wiley-Interscience Publication, 1980.

[45] M. K. Kadalbajoo and P. Arora, "B-spline collocation method for the singular-perturbation problem using artificial viscosity," Computers & Mathematics with Applications, vol. 57, no. 4, pp. 650–663, 2009.

[46] C. A. Hall, "On error bounds for spline interpolation," J Approx Theory, vol. 1, no. 2, pp. 209–218, 1968.

[47] C. de Boor, "On the convergence of odd-degree spline interpolation," J Approx Theory, vol. 1, no. 4, pp. 452–463, 1968.

[48] X. G. Zhu, Y. F. Nie, and W. Zhang, "An efficient differential quadrature method for fractional advection–diffusion equation," Nonlinear Dyn, vol. 90, pp. 1807–1827, 2017.